PROCEEDINGS OF SCIENCE

X-shape magnetic fields in galactic halos

Katia Ferrière*
IRAP, Université de Toulouse, CNRS - Toulouse
E-mail: katia.ferriere@irap.omp.eu

Recent radio polarization observations of nearby edge-on spiral galaxies have revealed the presence of X-shape magnetic fields in their halos. Whether the halo of our own Galaxy also hosts an X-shape magnetic field is still an open question, as such a field would be very hard to detect from inside. In this paper, I propose a mathematical description of X-shape magnetic fields, which can be used for fitting purposes or as inputs to various theoretical studies – including that of cosmic-ray propagation in galaxies.

Cosmic Rays and the InterStellar Medium - CRISM 2014,
24-27 June 2014
Montpellier, France

*Speaker.

PoS(CRISM2014)037

1. Introduction

Low-frequency radio waves provide the best observational tool to probe interstellar magnetic fields in galaxies. In the disks of external spirals, magnetic fields have long been observed to be generally horizontal (parallel to the disk plane) and to follow a spiral pattern, while in the halos of external edge-on spirals, they were recently found to possess an overall X shape, with a vertical component (perpendicular to the disk plane) that increases with both galactic radius and height in the four quadrants (see, e.g., [7, 5, 2] for recent reviews).

Several physical scenarios have been put forward to explain the origin of X-shape magnetic fields in galactic halos (see [4]). The first class of scenarios rests on the hypothesis that the X shape pertains to the large-scale regular magnetic field. Under this hypothesis, the simplest possibility would be that the X shape is produced by a conventional galactic dynamo operating in the halo [12, 9]. However, conventional dynamo fields do not naturally come with an X shape. To overcome this difficulty, a large-scale galactic wind has been invoked [12, 1, 6, 10] – either a wind originating near the galactic plane and advecting the disk dynamo field into the halo, or a wind blowing from the base of the halo and stretching out the halo dynamo field into an X shape [4]. In the second class of scenarios, the X shape pertains to a small-scale anisotropic random field. For instance, a spiky wind [3] could create extremely elongated magnetic loops that would line up with the local effective gravity (Michał Hanasz, private communication).

Independent of the question of their physical origin, a mathematical description of X-shape magnetic fields is often needed – for instance, to construct synthetic maps of rotation measures or synchrotron emission, or to study theoretical problems such as cosmic-ray propagation. The purpose of this paper is to provide simple descriptive equations that are both handy and consistent with the magnetic field divergence-free condition.

2. Magnetic field models

In this section, I present the four analytical models that [4] constructed to describe X-shape magnetic fields in galactic halos. Each of these models is initially defined by the shape of its field lines together with the distribution of the magnetic flux density on a given reference surface. Using the Euler formalism [8, 11], [4] derived the corresponding analytical expression of the magnetic field vector, (B_r, B_φ, B_z), as a function of galactocentric cylindrical coordinates, (r, φ, z).

In models A and B, a fixed reference radius, r_1, is introduced, and field lines are labeled by the height, z_1, and the azimuthal angle, φ_1, at which they cross the vertical cylinder of radius r_1. In models C and D, a fixed reference height, z_1, is introduced (more exactly, one reference height, $z_1 = 0$, in model C where all field lines cross the galactic midplane, and two reference heights, $z_1 = \pm|z_1|$, in model D where field lines do not cross the midplane), and field lines are labeled by the radius, r_1, and the azimuthal angle, φ_1, at which they cross the horizontal plane (or one of the two horizontal planes) of height z_1. Thus, the point (r_1, φ_1, z_1) of a given field line can be regarded as its footpoint on the reference surface (vertical cylinder of radius r_1 in models A and B and horizontal plane(s) of height z_1 in models C and D).

2.1 Poloidal field

The four models are distinguished by the shape of field lines associated with the poloidal field (hereafter referred to as the poloidal field lines), and hence by the expressions of the radial and vertical field components.

2.1.1 Models A and B

In **model A**, the shape of poloidal field lines is described by the quadratic function

$$z = z_1 \, \frac{1+a\,r^2}{1+a\,r_1^2} \, , \tag{2.1}$$

where a is a free parameter governing the opening of field lines away from the z-axis, r_1 is the prescribed reference radius and z_1 is the vertical label of the considered field line (see Fig. 1a). Conversely, the vertical label of the field line passing through (r,φ,z) is given by

$$z_1 = z \, \frac{1+a\,r_1^2}{1+a\,r^2} \, . \tag{2.2}$$

It then follows (see [4] for the detailed derivation) that the radial and vertical field components can be written as

$$B_r \, = \, \frac{r_1}{r} \, \frac{z_1}{z} \, B_r(r_1,\varphi_1,z_1) \tag{2.3}$$

$$B_z \, = \, \frac{2\,a\,r_1\,z_1}{1+a\,r^2} \, B_r(r_1,\varphi_1,z_1) \, , \tag{2.4}$$

with, for instance, $B_r(r_1,\varphi_1,z_1)$ obeying Eq. (2.9).

In **model B**, the corresponding equations read

$$z = \frac{1}{n+1} \, z_1 \, \left[\left(\frac{r}{r_1} \right)^{-n} + n \, \frac{r}{r_1} \right] \, , \tag{2.5}$$

with n a power-law index satisfying the constraint $n \geq 1$ (see Fig. 1b),

$$z_1 = (n+1) \, z \, \left[\left(\frac{r}{r_1} \right)^{-n} + n \, \frac{r}{r_1} \right]^{-1} \, , \tag{2.6}$$

and

$$B_r \, = \, \frac{r_1}{r} \, \frac{z_1}{z} \, B_r(r_1,\varphi_1,z_1) \tag{2.7}$$

$$B_z \, = \, -\frac{n}{n+1} \, \frac{r_1 \, z_1^2}{r^2 \, z} \, \left[\left(\frac{r}{r_1} \right)^{-n} - \frac{r}{r_1} \right] \, B_r(r_1,\varphi_1,z_1) \, . \tag{2.8}$$

In both **models A and B**, the radial field component on the vertical cylinder of radius r_1 is chosen to have a linear-exponential variation with z_1 and a sinusoidal variation with φ_1:

$$B_r(r_1,\varphi_1,z_1) = B_1 \, f_{\rm sym} \, \left[\frac{|z_1|}{H} \, \exp\left(-\frac{|z_1|-H}{H} \right) \right] \, \cos\Big(m \, \big(\varphi_1 - \varphi_\star(z_1) \big) \Big) \, , \tag{2.9}$$

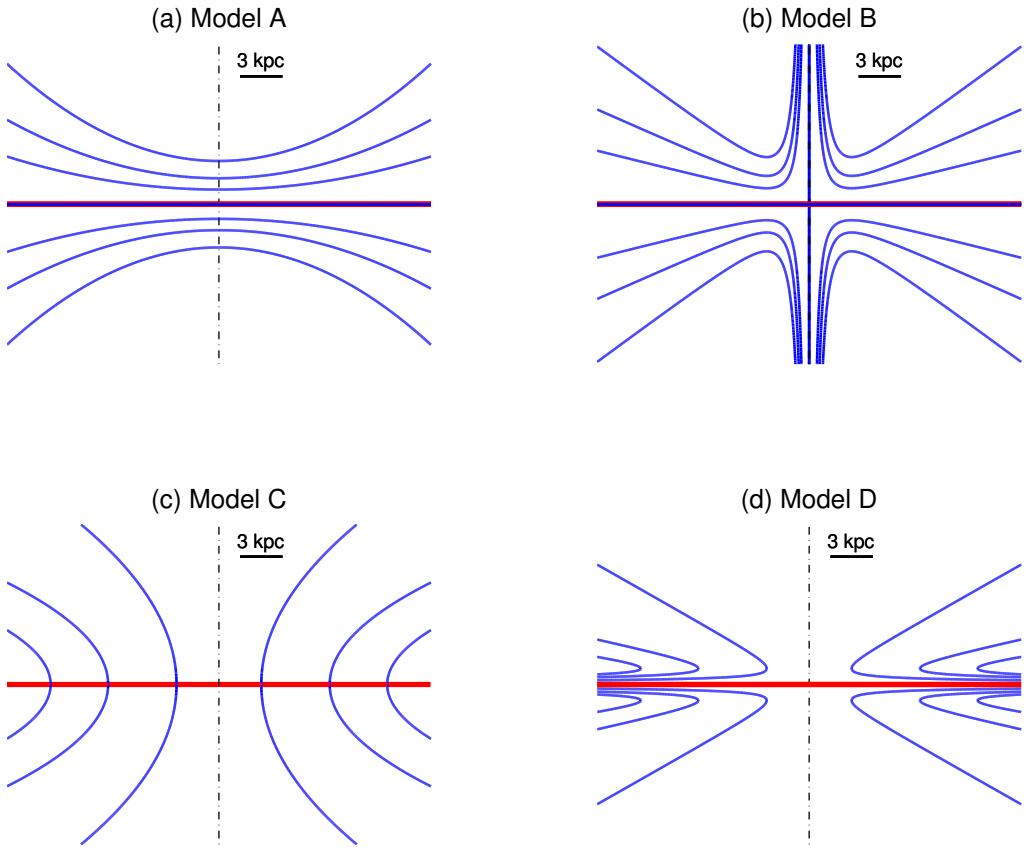

Figure 1: Sample of field lines for each of the four models of poloidal fields, in a vertical plane through the galactic center: (a) model A with $r_1 = 3$ kpc and $a = 1/(10\ \mathrm{kpc})^2$; (b) model B with $r_1 = 3$ kpc and $n = 2$; (c) model C with $a = 1/(10\ \mathrm{kpc})^2$ (and, as always, $z_1 = 0$); and (d) model D with $|z_1| = 1.5$ kpc and $n = 2$. Each panel is 30 kpc $\times$ 30 kpc in size, with the trace of the galactic plane indicated by the horizontal, red, solid line, and the z-axis by the vertical, black, dot-dashed line.

where B_1 is the normalization field, f_{sym} is a factor setting the vertical parity of the magnetic field[1] ($f_{\mathrm{sym}} = 1$ for symmetric fields and $f_{\mathrm{sym}} = \mathrm{sign}\ z_1$ for antisymmetric fields), H is the exponential scale height, m is the azimuthal wavenumber and $\varphi_\star(z_1)$ the fiducial angle of the azimuthal modulation.

2.1.2 Models C and D

Models C and D are the direct counterparts of models A and B, respectively, with the roles of the coordinates r and z inverted in the equation of field lines.

In **model C**, the reference height is set to $z_1 = 0$, and the shape of poloidal field lines is described by the quadratic function

$$r = r_1\ (1 + a z^2)\ , \tag{2.10}$$

[1] A magnetic field is symmetric/antisymmetric with respect to the galactic midplane (or quadrupolar/dipolar) when its horizontal components, B_r and B_φ, are even/odd functions of z and its vertical component, B_z, is an odd/even function of z.

with a a free parameter governing the opening of field lines away from the r-axis and r_1 the radial label of the considered field line (see Fig. 1c). Conversely, the radial label of the field line passing through (r,φ,z) is given by

$$r_1 = \frac{r}{1+az^2} \cdot \tag{2.11}$$

The radial and vertical field components can then be written as

$$B_r = \frac{2ar_1^3 z}{r^2} B_z(r_1,\varphi_1,z_1) \tag{2.12}$$

$$B_z = \frac{r_1^2}{r^2} B_z(r_1,\varphi_1,z_1) \,, \tag{2.13}$$

with, for instance, $B_z(r_1,\varphi_1,z_1)$ obeying Eq. (2.18).

In **model D**, where every field line remains confined to one side of the galactic midplane, a reference height, $z_1 = |z_1|$ sign z, is prescribed on each side of the midplane, such that the ratio (z/z_1) is always positive. We then have

$$r = \frac{1}{n+1} r_1 \left[\left(\frac{z}{z_1} \right)^{-n} + n \frac{z}{z_1} \right] \,, \tag{2.14}$$

with $n \geq \frac{1}{2}$ (see Fig. 1d),

$$r_1 = (n+1)\, r \left[\left(\frac{z}{z_1} \right)^{-n} + n \frac{z}{z_1} \right]^{-1} \,, \tag{2.15}$$

and

$$B_r = -\frac{n}{n+1} \frac{r_1^3}{r^2 z} \left[\left(\frac{z}{z_1} \right)^{-n} - \frac{z}{z_1} \right] B_z(r_1,\varphi_1,z_1) \tag{2.16}$$

$$B_z = \frac{r_1^2}{r^2} B_z(r_1,\varphi_1,z_1) \cdot \tag{2.17}$$

In both **models C and D**, the vertical field component on the horizontal plane(s) of height z_1 is chosen to have an exponential variation with r_1 and a sinusoidal variation with φ_1:

$$B_z(r_1,\varphi_1,z_1) = B_1 \, f_{\rm sym} \, \exp\left(-\frac{r_1}{L}\right) \cos\Big(m\left(\varphi_1 - \varphi_\star(r_1)\right)\Big) \,, \tag{2.18}$$

with B_1 the normalization field, $f_{\rm sym}$ a factor setting the vertical parity of the magnetic field ($f_{\rm sym} = 1$ in model C, which is always antisymmetric, and in the antisymmetric version of model D, and $f_{\rm sym} = \text{sign}\, z_1$ in the symmetric version of model D), L the exponential scale length, m the azimuthal wavenumber and $\varphi_\star(r_1)$ the fiducial angle of the azimuthal modulation.

2.2 Azimuthal field

In all four models, field lines are assumed to spiral up or down (see Fig. 2) according to the equation

$$\varphi = \varphi_1 + f_\varphi(r,z) \,, \tag{2.19}$$

where $f_\varphi(r,z)$ is a winding function which vanishes on the reference surface ($f_\varphi(r_1,z_1)=0$) and decreases or increases monotonically away from it. The field line passing through (r,φ,z) can then be traced back to the azimuthal label

$$\varphi_1 = \varphi - f_\varphi(r,z) \cdot \tag{2.20}$$

In practice, it is often more convenient to describe the spiraling of field lines with the pitch angle, $p(r,z)$, defined as the angle between the tangent to the field line projection onto the galactic plane and the local azimuthal direction:

$$\cot p = \frac{r\,d\varphi}{dr} = r\,\frac{df_\varphi}{dr}\ , \tag{2.21}$$

where the derivative with respect to r is to be taken along field lines. The simplest possible choice for the pitch angle is a constant value, which leads to a logarithmic spiral with $f_\varphi(r,z) = \cot p\ \ln(r/r_1)$. Another simple choice, which reflects the expected increase of the pitch angle with increasing height, is

$$p(r,z) = p_\infty + (p_0 - p_\infty)\ \left(1+\left(\frac{|z|}{H_p}\right)^2\right)^{-1}\ , \tag{2.22}$$

with p_0 the pitch angle at midplane, p_∞ the pitch angle at infinity and H_p the scale height.

For a given pitch angle distribution, the winding function is obtained by integrating Eq. (2.21) along field lines:

$$f_\varphi(r,z) = \int_{r_1}^{r} \cot p(r',z')\ \frac{1}{r'}\ dr' \tag{2.23}$$

or, equivalently,

$$f_\varphi(r,z) = \int_{z_1}^{z} \cot p(r',z')\ \left(\frac{1}{r'}\,\frac{dr'}{dz'}\right)\ dz'\ , \tag{2.24}$$

where z' is the height of the considered field line at radius r'.

In **models A and B**, where poloidal field lines are defined by z as a function of r, it is more appropriate to use Eq. (2.23), with z' inferred from Eq. (2.1) in model A:

$$z' = z\,\frac{1+a\,r'^2}{1+a\,r^2}\ , \tag{2.25}$$

and z' inferred from Eq. (2.5) in model B:

$$z' = z\,\frac{\left(\dfrac{r'}{r_1}\right)^{-n} + n\,\dfrac{r'}{r_1}}{\left(\dfrac{r}{r_1}\right)^{-n} + n\,\dfrac{r}{r_1}}\ \cdot \tag{2.26}$$

In contrast, in **models C and D**, where poloidal field lines are defined by r as a function of z, it is more appropriate to use Eq. (2.24), with r' inferred from Eq. (2.10) in model C:

$$r' = r\,\frac{1+a\,z'^2}{1+a\,z^2} \tag{2.27}$$

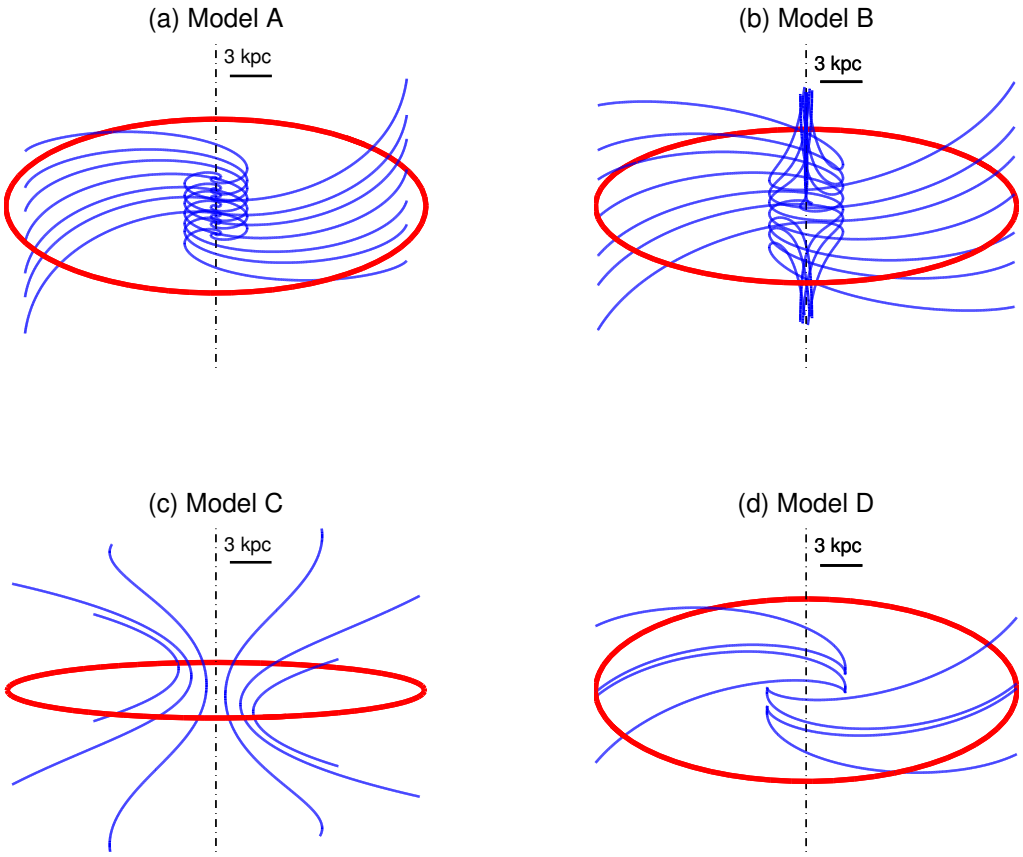

Figure 2: Sample of field lines for each of the four complete magnetic field models, as seen from an oblique angle. The parameters of the poloidal field have the same values as in Fig. 1, while the pitch angle is set to $p = -30°$. The selected field lines are the wound-up versions of the field lines displayed in Fig. 1 (except in model D, where fewer field lines are drawn for clarity). Each box is a $(30\ \mathrm{kpc})^3$ cube, with the galactic plane traced by the red, solid circle, and the z-axis by the vertical, black, dot-dashed line.

and

$$\left(\frac{1}{r'}\,\frac{dr'}{dz'}\right) = \frac{2\,a\,z'}{1+a\,z'^2}\ , \tag{2.28}$$

and r' inferred from Eq. (2.14) in model D:

$$r' = r\,\frac{\left(\dfrac{z'}{z_1}\right)^{-n} + n\,\dfrac{z'}{z_1}}{\left(\dfrac{z}{z_1}\right)^{-n} + n\,\dfrac{z}{z_1}} \tag{2.29}$$

and

$$\left(\frac{1}{r'}\,\frac{dr'}{dz'}\right) = -n\,\frac{1}{z'}\,\frac{\left(\dfrac{z'}{z_1}\right)^{-n} - \dfrac{z'}{z_1}}{\left(\dfrac{z'}{z_1}\right)^{-n} + n\,\dfrac{z'}{z_1}}\ . \tag{2.30}$$

Since the magnetic field is by definition tangent to field lines, the pitch angle also represents the angle between the horizontal field and the local azimuthal direction, so that the azimuthal component of the field is related to its radial component through

$$B_\varphi = \cot p \, B_r \cdot \tag{2.31}$$

3. Summary

In this paper, I presented four analytical models of X-shape magnetic fields in galactic halos. The poloidal field is described by Eqs. (2.3) – (2.4) in model A, Eqs. (2.7) – (2.8) in model B, Eqs. (2.12) – (2.13) in model C, and Eqs. (2.16) – (2.17) in model D, while the azimuthal field is described by Eq. (2.31), with, for instance, Eq. (2.22), in all models. Together, these equations relate the magnetic field at an arbitrary point (r,φ,z) to the field component normal to the reference surface (vertical cylinder of radius r_1 in models A and B and horizontal plane(s) of height z_1 in models C and D) at the footpoint (r_1,φ_1,z_1) on the reference surface of the field line passing through (r,φ,z). The footpoint, in turn, is determined by the reference coordinate (r_1 in models A and B and z_1 in models C and D), the poloidal label of the field line (Eq. (2.2) in model A, Eq. (2.6) in model B, Eq. (2.11) in model C, Eq. (2.15) in model D), and its azimuthal label (Eq. (2.20) in all models).

An important remark must be made regarding model A. As can be seen from Fig. 1a, all field lines, from all meridional planes, converge to the z-axis, so that $B_r \to \infty$ for $r \to 0$ (see Eq. (2.3)). In reality, this unphysical behavior poses an insuperable problem only in the axisymmetric case. In non-axisymmetric configurations, a slight modification of the magnetic topology near the z-axis may be sufficient to remove the singularity.

References

[1] Beck, R. 2008, American Institute of Physics Conference Series, Vol. 1085, eds. F. A. Aharonian, W. Hofmann, & F. Rieger, 83

[2] Beck, R. & Wielebinski, R. 2013, Magnetic Fields in Galaxies, Planets, Stars and Stellar Systems, Vol. 5, eds. T. D. Oswalt & G. Gilmore (Dordrecht: Springer Science, Business Media), 641

[3] Elstner, D., Golla, G., Rudiger, G., & Wielebinski, R. 1995, A&A, 297, 77

[4] Ferrière, K. & Terral, P. 2014, A&A, 561, A100

[5] Haverkorn, M. & Heesen, V. 2012, Space Science Reviews, 166, 133

[6] Heesen, V., Krause, M., Beck, R., & Dettmar, R.-J. 2009, A&A, 506, 1123

[7] Krause, M. 2009, Revista Mexicana de Astronomia y Astrofisica Conference Series, Vol. 36, 25

[8] Northrop, T. G. 1963, Reviews of Geophysics and Space Physics, 1, 283

[9] Soida, M. 2005, The Magnetized Plasma in Galaxy Evolution, eds. K. T. Chyzy, K. Otmianowska-Mazur, M. Soida, & R.-J. Dettmar (Kraków: Jagiellonian University), 185

[10] Soida, M., Krause, M., Dettmar, R.-J., & Urbanik, M. 2011, A&A, 531, A127

[11] Stern, D. P. 1966, Space Science Reviews, 6, 147

[12] Tüllmann, R., Dettmar, R.-J., Soida, M., Urbanik, M., & Rossa, J. 2000, A&A, 364, L36